Supporting Information

Rational design of Metal-Organic Framework Derived ZnFe2O4/ Fe2O3 Modified Carbon Cloth with intermittent lithiophilicity for High-Performance Anode-Free Lithium Metal Batteries

Xiaonuo Jiang [a], Xingtong Guo [a], Rui Luo [a], Zi Wang [a], Hongmei Cao [a,*], Tao Wei [a,*]

[a] *School of Energy and Power, Jiangsu University of Science and Technology, Zhenjiang 212100, China.*

Experimental section

Preparation of CC@$ZnFe_2O_4/Fe_2O_3$

Firstly, 0.5 mmol of $FeCl_3$, 1.5 mmol of $ZnCl_2$, and 2 mmol of 2-aminoterephthalic acid (NH_2-BDC) were mixed in a solution containing 25 mL of dimethylformamide (DMF) and 25 mL of ethanol. Subsequently, 2 mL of 0.4 mol L^{-1} NaOH aqueous solution was added. Cleaned CC discs were then immersed into the mixture, which was subjected to ultrasonication for 15 minutes followed by stirring at room temperature for 30 minutes. The resulting mixture was transferred to an autoclave and reacted at 150 ℃ for 6 h. Then, the product was collected after washed with deionized water and dried at 80 ℃ for 6 h. Finally, the product was calcined in an oxygen atmosphere at 450 ℃ for 2 h with a heating rate of 2 ℃ min^{-1} to obtain CC@$ZnFe_2O_4/Fe_2O_3$.

* Corresponding author: H. Cao (caohm@just.edu.cn).

* Corresponding author: T. Wei (wt863@just.edu.cn; wt863@126.com).

Materials characterizations

The crystal structure of ZnFe-MOFs and ZnFe-MOFs derivatives samples were characterized by using X-ray diffraction (XRD) over a range of 10° to 70° at 10° min^{-1}. The surface morphologies of pure CC, CC@ZnFe-MOFs, and CC@$ZnFe_2O_4/Fe_2O_3$ were observed by scanning electron microscope (SEM). Elemental compositions of ZnFe-MOFs and ZnFe-MOF derivatives were investigated via X-ray photoelectron spectroscopy (XPS). Additionally, the elemental distribution uniformity of the CC@$ZnFe_2O_4/Fe_2O_3$ was observed through energy-dispersive X-ray spectroscopy (EDS). The surface morphology of the ZnFe-MOF derivatives was observed by transmission electron microscopy (TEM), while their internal structure was investigated using high-resolution TEM (HRTEM).

Electrochemical measurements

The electrochemical performance of the CC@$ZnFe_2O_4/Fe_2O_3$ composite was evaluated using CR2032 coin cells. The electrolyte consisted of 1.0 M LiTFSI in an equal-volume mixture of 1,3-dioxolane (DOL) and 1,2-dimethoxyethane (DME), supplemented with 1.0 wt% $LiNO_3$. This electrolyte formulation was employed for both symmetrical cell cycling and Coulombic efficiency (CE) tests. For full-cell assembly, a cathode slurry was prepared by mixing 70 wt% $LiFePO_4$ (LFP), 20 wt% acetylene black, and 10 wt% polyvinylidene fluoride (PVDF) in N-methyl-2-pyrrolidone (NMP). The slurry was uniformly coated onto an aluminum current collector, dried at 60 ℃ for 3 h, and then further dried overnight at 120 ℃ under vacuum. Circular electrodes with a diameter of 14 mm were punched from the dried film. The mass range of the compacted working electrodes was about 8.0 mg (4.88 mg cm^{-2}) to 18.9 mg (12.3 mg cm^{-2}). For anode-free full cells, the cathode employed was a high-loading $LiFePO_4$

(LFP: 12.3 mg cm^{-2}), and the anode was CC@$ZnFe_2O_4/Fe_2O_3$ without any additional Li source. The electrolyte used in full cells was 1.0 M $LiPF_6$ dissolved in a mixture of ethylene carbonate (EC), dimethyl carbonate (DMC), and ethyl methyl carbonate (EMC) with a volume ratio of 1:1:1. The electrolyte volume was 30 μL, corresponding to an E/C ratio of 11.54 μL mAh^{-1}. All cells were assembled in argon-filled glove box (H_2O and O_2 levels < 0.1 ppm) using Celgard 2500 as the separator. Galvanostatic charge-discharge tests were conducted on the Land Battery Testing Systems at room temperature (26 ℃) with a 12 h rest period before testing. For full cells, the voltage range was 2.6-4.0 V and the rate ranged from 0.2 to 10 C. Cyclic voltammetry (CV) and electrochemical impedance spectroscopy (EIS) measurements were performed on a CHI-660E electrochemical workstation. EIS spectra were recorded from 100 kHz to 0.01 Hz with an AC amplitude of 5 mV. CV scans were carried out at a rate of 0.2 mV s^{-1} within a voltage window of 2.4-4.0 V.

Experimental data

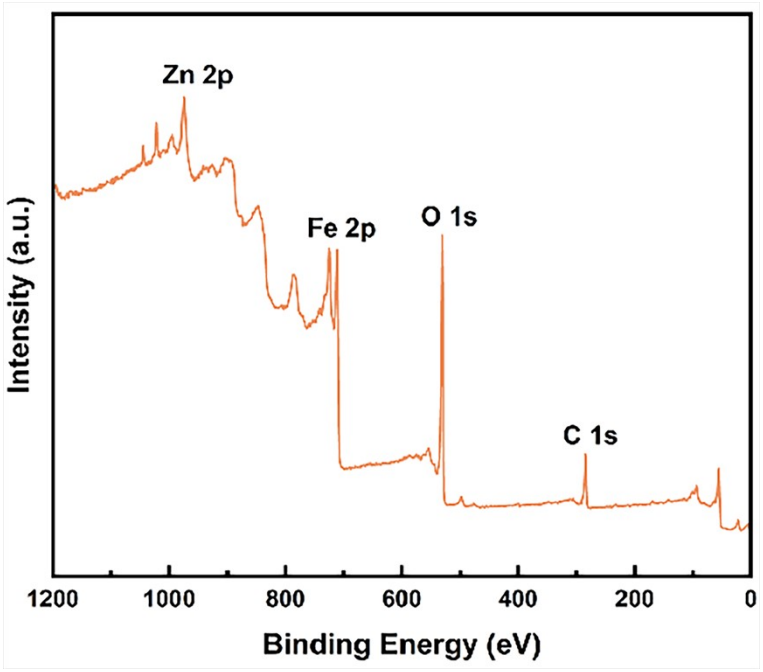

Fig. S1 Full XPS spectrum of ZnFe-MOFs derivatives.

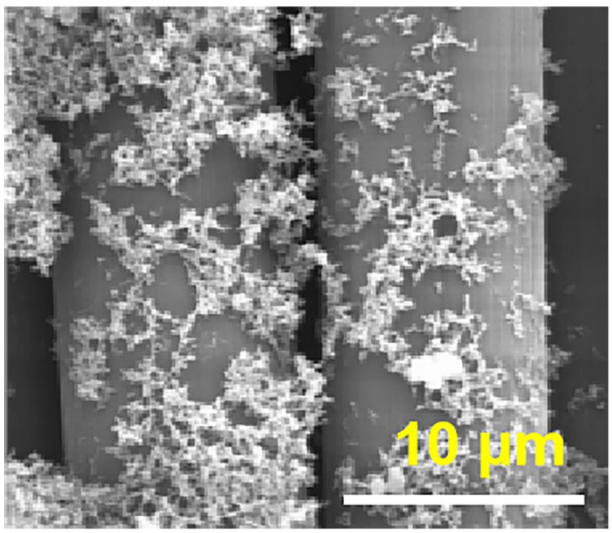

Fig. S2 SEM image of the CC@$ZnFe_2O_4/Fe_2O_3$@Li.

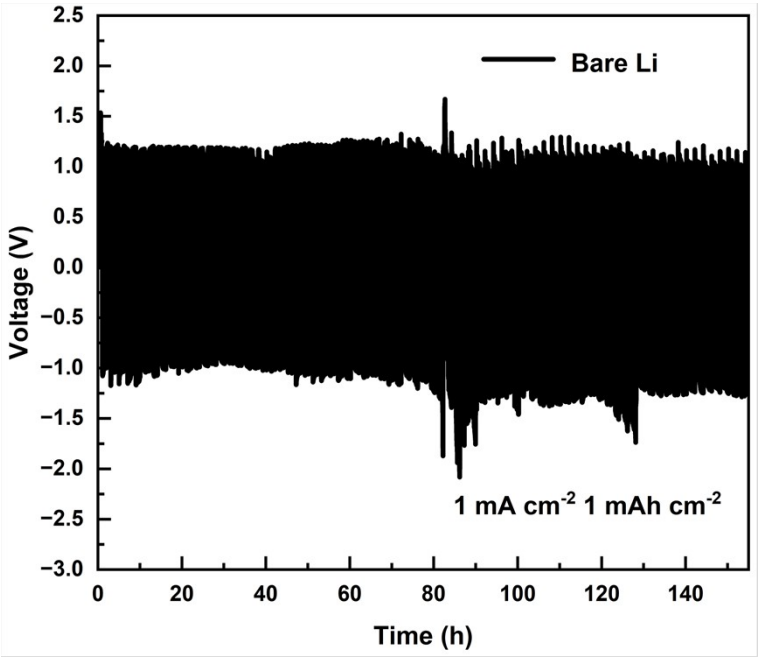

Fig. S3 Long-term cycling performance of symmetric cells with bare Li electrodes at 1 mA cm^{-2}, 1 mAh cm^{-2}.

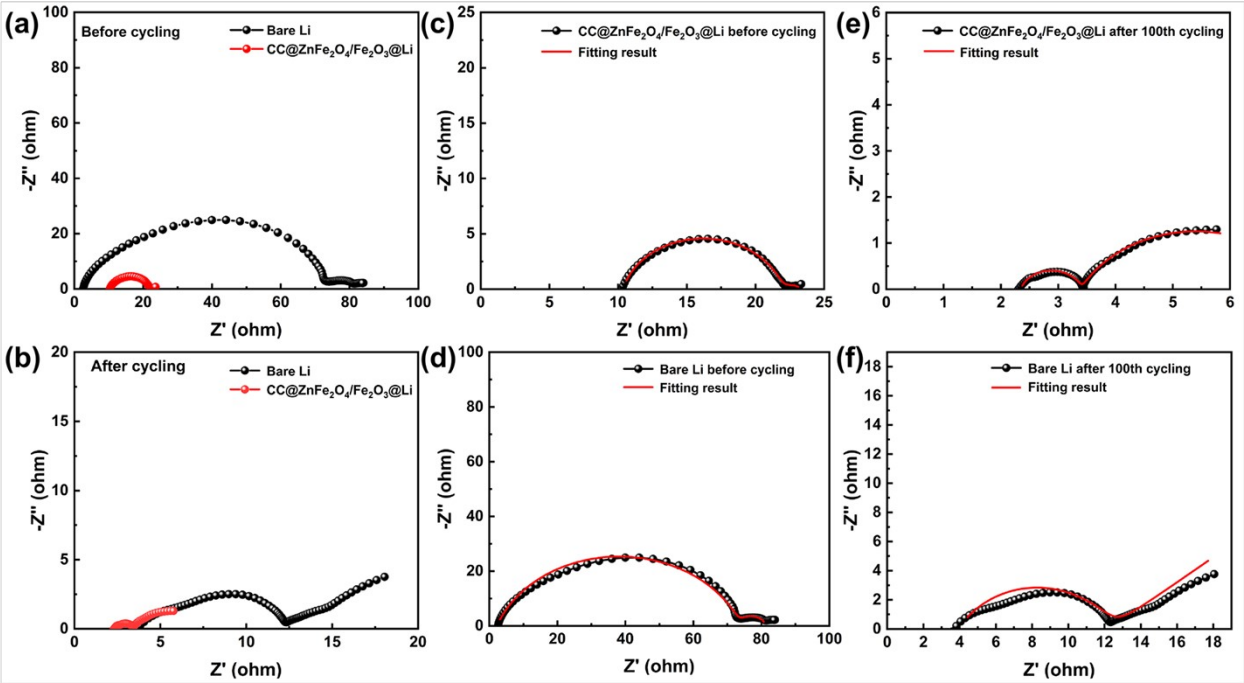

Fig. S4 Nyquist plots of the impedance spectra of Li||Li and CC@$ZnFe_2O_4$/Fe_2O_3@Li||CC@$ZnFe_2O_4$/Fe_2O_3@Li symmetric cells (a) before cycling, and (b) after cycling. Nyquist plots and their corresponding fitted curves of CC@$ZnFe_2O_4$/Fe_2O_3@Li||CC@$ZnFe_2O_4$/Fe_2O_3@Li and Li||Li symmetric cells (c, d) before cycling, and (e, f) after cycling.

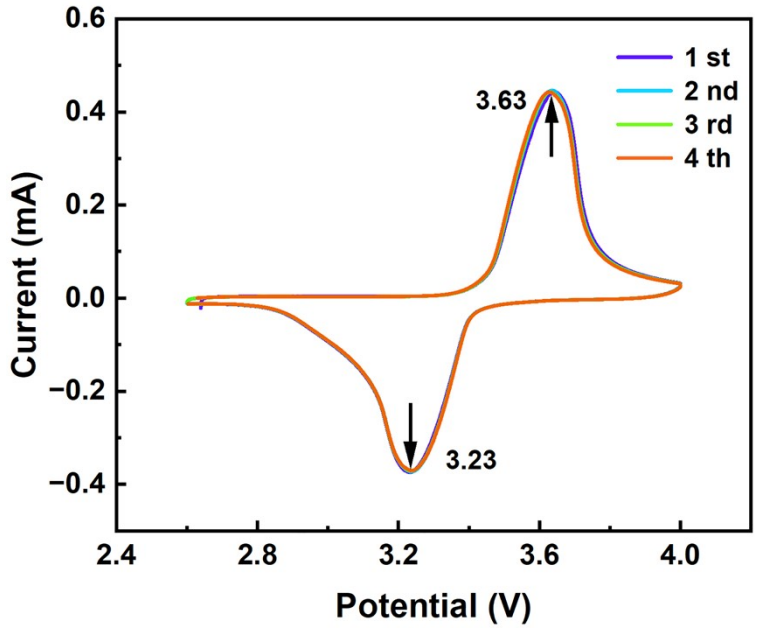

Fig. S5 CV curves of CC@$ZnFe_2O_4$/Fe_2O_3@Li||LFP full cell.

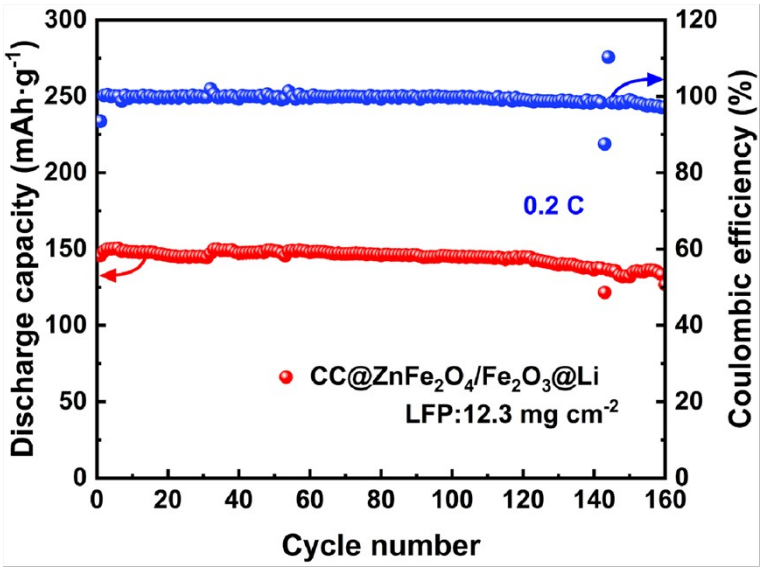

Fig. S6 Long-term cycling performance of the CC@$ZnFe_2O_4/Fe_2O_3$@Li||LFP full cell at 0.2 C (LFP: 12.3 mg cm^{-2}).

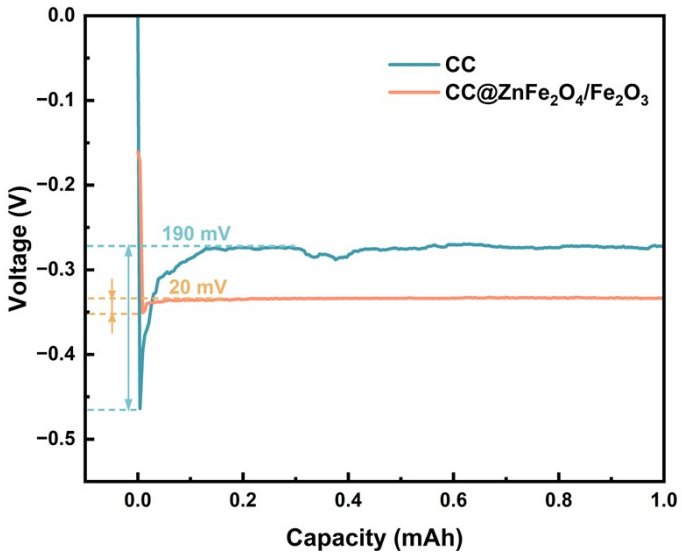

Fig. S7 First discharge profiles of Li||CC and Li||CC@$ZnFe_2O_4/Fe_2O_3$ half cells.

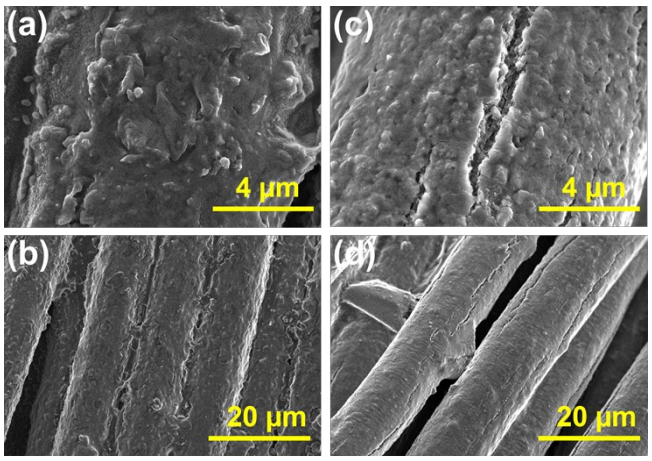

Fig. S8 The SEM images of the CC electrodes after lithium deposition for different time at 1 mA cm^{-2}: (a, b) 1 h, (c, d) 3 h

Fig. S9 Calculation of binding energy of Li with graphitic carbon.

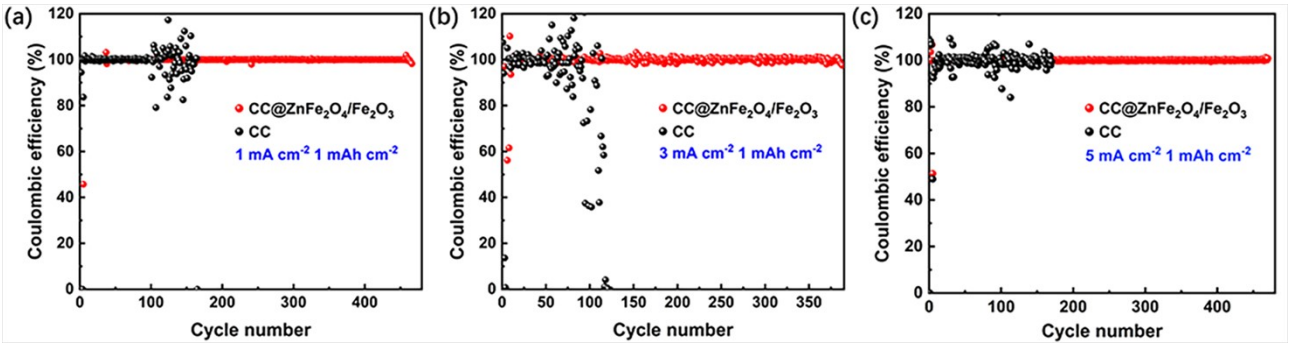

Fig. S10 Coulombic efficiency (CE) of the CC@$ZnFe_2O_4/Fe_2O_3$ and CC electrodes at a capacity of 1 mAh cm^{-2} and current densities of (a) 1 mA cm^{-2}, (b) 3 mA cm^{-2}, and (c) 5 mA cm^{-2}.

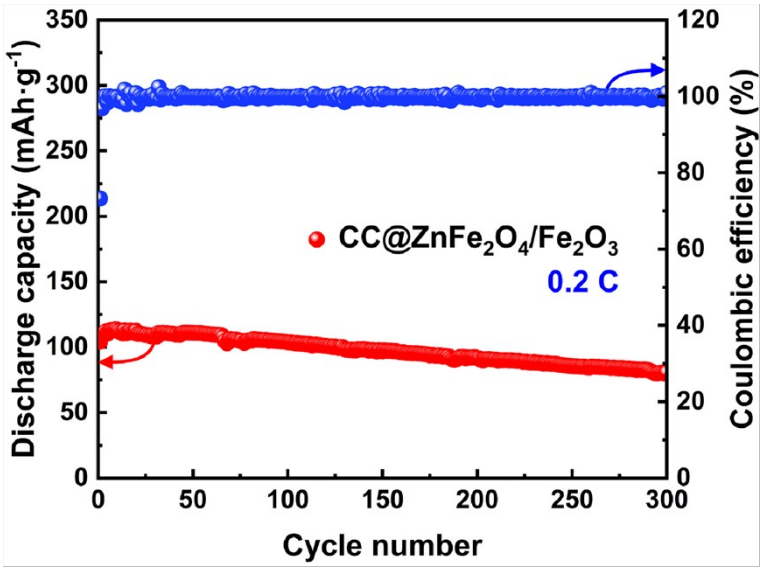

Fig. S11 Long-term cycling performance of CC@$ZnFe_2O_4/Fe_2O_3$||LFP full cells at 0.2 C (LFP: 12.3 mg cm^{-2}).

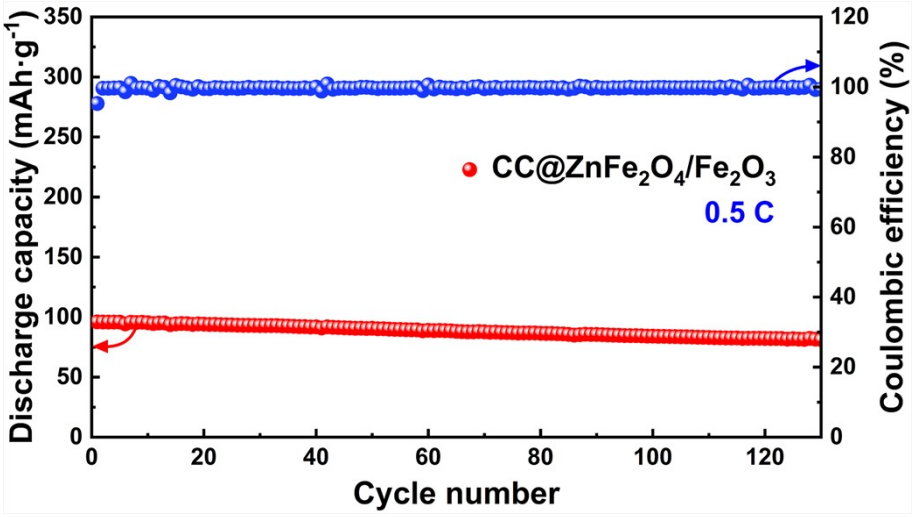

Fig. S12 Long-term cycling performance of CC@$ZnFe_2O_4/Fe_2O_3$||LFP full cells at 0.5 C (LFP: 12.3 mg cm^{-2}).

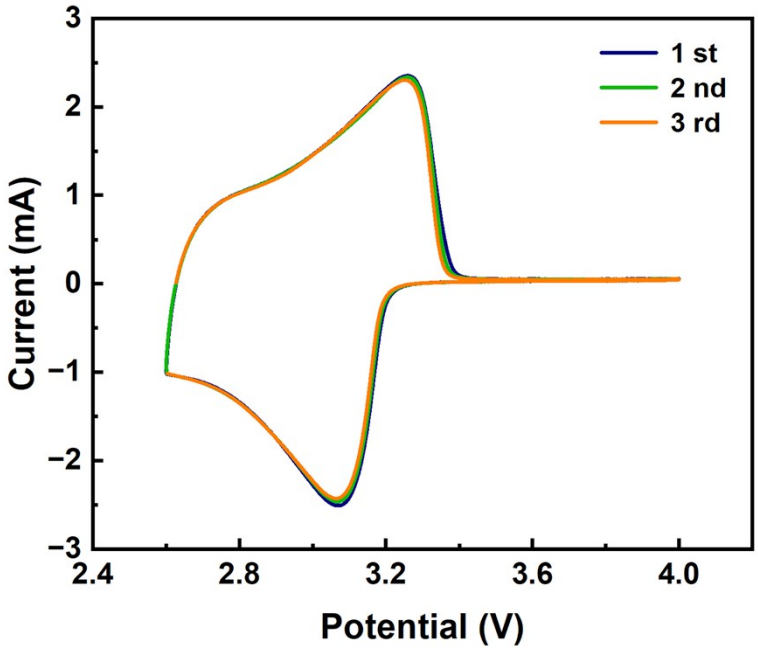

Fig. S13 CV curve of CC@$ZnFe_2O_4/Fe_2O_3$||LFP full cells.

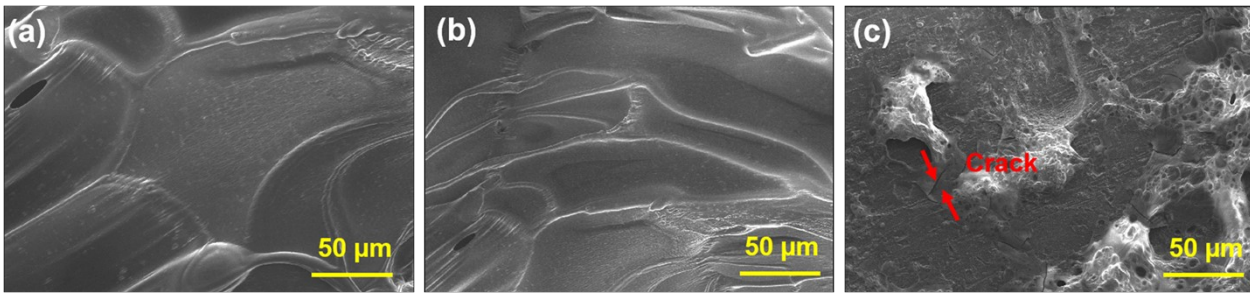

Fig. S14 SEM images of the (a) CC@$ZnFe_2O_4/Fe_2O_3$@Li, (b) CC@$ZnFe_2O_4/Fe_2O_3$, and (c) bare Li electrodes after 100 cycles at 1 C in full cells.

Table S1. Electrochemical impedance fitting results of symmetric cells with different electrodes.

Electrode	R_s / Ω	R_{int} / Ω	R_{total}/ Ω
Li foil (before)	2.43	79.56	81.99
CC@$ZnFe_2O_4$/Fe_2O_3@Li (before)	10.37	13.06	23.43
Li foil (after)	3.91	8.42	12.33
CC@$ZnFe_2O_4$/Fe_2O_3@Li (after)	2.35	4.99	7.34

Table S2. Summary of the cycling performance of AFLMBs with different current collector modification strategies

Anode	Electrolyte	Current Density	Cycle number	Capacity retention	Ref.
CC@$ZnFe_2O_4$/Fe_2O_3	**1.0 M $LiPF_6$ in EC:DMC:EMC (1:1:1 wt%)**	**0.5 C 2 C**	**130 1000**	**85% 81%**	**This work**
MXene@Ag	1.0 M LiTFSI in DOL/DME (v/v = 1:1) with 1 wt % $LiNO_3$	0.5 C	110	-	1
Cu@CC3	1.0 M LiTFSI in DOL/DME (v/v = 1:1) with 3 wt % $LiNO_3$	0.33 C	100	75%	2
P-Cu	1.0 M LiTFSI in DOL/DME with 5 wt % $LiNO_3$	1 C	80	-	3
Zn_3N_2@Cu	1.0 M LiTFSI in DOL/DME (v/v = 1:1) with 1 wt % $LiNO_3$	0.5 C	100	63.1%	4
$AgCu_x$-400	1.0 M $LiPF_6$ in EC:DMC:EMC (1:1:1 wt%)	1 mA cm^{-2}	100	-	5
Sn@Cu	1.0 M $LiPF_6$ in EC/DEC (v/v = 1:1)	0.1 C	90	47.5%	6
Cu-10	1.0 M LiTFSI in DOL/DME (v/v = 1:1) with 2 wt % $LiNO_3$	0.5 C	100	43%	7
a-RF@3D-CM	1 M LiTFSI in DOL/DME with 2 wt% $LiNO_3$	0.2 C	100	60.66%	8
TSCG	1.0 M $LiPF_6$ in EC/DMC	0.3 C	800	87%	9
PI@Au	1.0 M LiTFSI in DOL/DME (v/v = 1:1) with 2 wt % $LiNO_3$	0.5 mA cm^{-2}	350	18.2%	10

References

1 C. Wang, C. Yang, Y. Du, Z. Guo and H. Ye, *Adv. Funct. Mater.*, 2023, **33**, 2303427.
2 J. Xu, K. Qu, X. Li, Y. Cui, J. Li, H. Liu and C. Lian, *ACS Nano*, 2025, **19**, 2936–2943.
3 Z. Sun, Y. Wang, Y. Qin, P. Yang, H. Wu, X. Li, X. Hu, C. Xiao, H. Zhao, M. Ma, Y. Su and S. Ding, *Energy Storage Mater.*, 2023, **58**, 110–122.
4 Y. Zhu, S. Wu, L. Zhang, B. Zhang and B. Liao, *ACS Appl. Mater. Interfaces*, 2023, **15**, 43145–43158.
5 H. Yu, P. Sun, H. Cheng, Z. Ding and D. Luo, *Electrochim. Acta*, 2025, **535**, 146623.
6 Y. Li, M. Bu, C. Mu and C. Yang, *Mater. Lett.*, 2024, **355**, 135449.
7 J. Chen, L. Dai, P. Hu and Z. Li, *Molecules*, 2023, **28**, 548.
8 N. Li, T. Jia, Y. Liu, Y. Ouyang, Y. Lv, G. Zhong, Y. Wang, B. Sun, S. Lu, S. Huang, F. Kang and Y. Cao, *Mater. Today Energy*, 2023, **36**, 101341.
9 Y. Li, J. Chen, P. Cai and Z. Wen, *J. Mater. Chem. A*, 2018, **6**, 4948–4954.
10 H. H. Weldeyohannes, L. H. Abrha, Y. Nikodimos, K. N. Shitaw, T. M. Hagos, C.-J. Huang, C.-H. Wang, S.-H. Wu, W.-N. Su and B. J. Hwang, *J. Power Sources*, 2021, **506**, 230204.